

# A numerical model for the simulation of the seismic cycle in tectonic settings in favor or against gravity: examples from Italy

Matteo Albano<sup>1</sup>, Salvatore Barba<sup>1</sup>, Christian Bignami<sup>1</sup>, Eugenio Carminati<sup>2</sup>, Carlo Doglioni<sup>2</sup>, Marco Moro<sup>1</sup>, Michele Saroli<sup>1</sup>, and Salvatore Stramondo<sup>1</sup>

<sup>1</sup>National Institute of Geophysics and Volcanology

<sup>2</sup>Sapienza University of Rome

November 21, 2022

## Abstract

According to the concept of the seismic cycle, earthquakes result from the strain accumulation over a variable decade to millennial period, i.e., the interseismic stage, followed by a sudden stress release, i.e., the coseismic stage, eventually evolving in the postseismic stage. Common analytical and numerical approaches simulate interseismic, coseismic and postseismic stages independently. Often, coseismic models constrain the slip of single or multiple planar sources to fit the available geodetic and InSAR measurements to reproduce fault geometry, slip and regional deformation, regardless the origin of the interseismic forces. We developed a numerical model linking the ongoing interseismic viscous deformation at depth with the coseismic brittle episodic behavior of the upper crust. Our model assumes a brittle upper crust where the fault is locked, and a ductile lower crust, where the fault is steadily shearing. This approach is developed to model typical extensional and compressional earthquakes in Italy including the forces acting during the interseismic period, i.e., the lithostatic load and the horizontal stress field. We adjusted the setup of our model to simulate the interseismic, coseismic and postseismic phases of three seismic events in Italy, two extensional (2009 L'Aquila Mw 6.1 and 2016 Amatrice-Norcia Mw 6.5) and one contractional (2012 Emilia Mw 6). The results of our analysis, compared with the available geodetic and InSAR data, show that the proposed numerical model can reproduce the seismic cycle associated with the investigated events. The modeling provides evidence of interseismic dilatancy above the brittle-ductile transition at the bottom of the locked fault plane in the extensional tectonic setting; coseismic fault motion is triggered by the hangingwall gravitational collapse that recovers most of the interseismic dilatancy formed almost orthogonal to the fault. Vice versa, in contractional tectonic settings, the interseismic horizontal stress accumulates elastic energy in the crustal volume above the bottom of the locked fault; coseismic deformation recovers the elastic energy stored in the hangingwall. The two different settings generate a deformation in favor of gravity in extensional tectonic environments and against gravity in contractional tectonic environments.

# A Numerical model for the simulation of the seismic cycle in tectonic settings in favor or against gravity: examples from Italy

Matteo Albano <sup>1\*</sup>, Salvatore Barba <sup>1</sup>, Christian Bignami <sup>1</sup>, Eugenio Carminati <sup>2</sup>, Carlo Doglioni <sup>1,2</sup>, Marco Moro <sup>1</sup>, Michele Saroli <sup>3</sup>, Salvatore Stramondo <sup>1</sup>

<sup>1</sup>Istituto Nazionale di Geofisica e Vulcanologia, Roma, Italy; <sup>2</sup>"Sapienza" Università di Roma, Roma, Italy; <sup>3</sup>Università degli Studi di Cassino e del Lazio Meridionale, Cassino, Italy; \*matteo.albano@ingv.it

## Abstract

According to the concept of the seismic cycle, earthquakes result from the strain accumulation over a variable decade to millennial period, i.e., the interseismic stage, followed by a sudden stress release, i.e., the coseismic stage, eventually evolving in the postseismic stage.

Common analytical and numerical approaches simulate interseismic, coseismic and postseismic stages independently. Often, coseismic models constrain the slip of single or multiple planar sources to fit the available geodetic and InSAR measurements to reproduce fault geometry, slip and regional deformation, regardless the origin of the interseismic forces.

We developed a numerical model linking the ongoing interseismic viscous deformation at depth with the coseismic brittle episodic behavior of the upper crust. Our model assumes a brittle upper crust where the fault is locked, and a ductile lower crust, where the fault is steadily shearing.

This approach is developed to model typical extensional and compressional earthquakes in Italy including the forces acting during the interseismic period, i.e., the lithostatic load and the horizontal stress field.

The results of our analysis, compared with the available geodetic and InSAR data, show that the proposed numerical model can reproduce the seismic cycle associated with the investigated events.

## Introduction

We simulated the interseismic and coseismic phases of three seismic events in Italy (Figure 1a), two extensional events: the 2009 L'Aquila, Mw 6.1 (Figure 1b) and the 2016 Amatrice-Norcia, Mw 6.5 (Figure 1c), and one contractional: the 2012 Emilia, Mw 6 (Figure 1d).

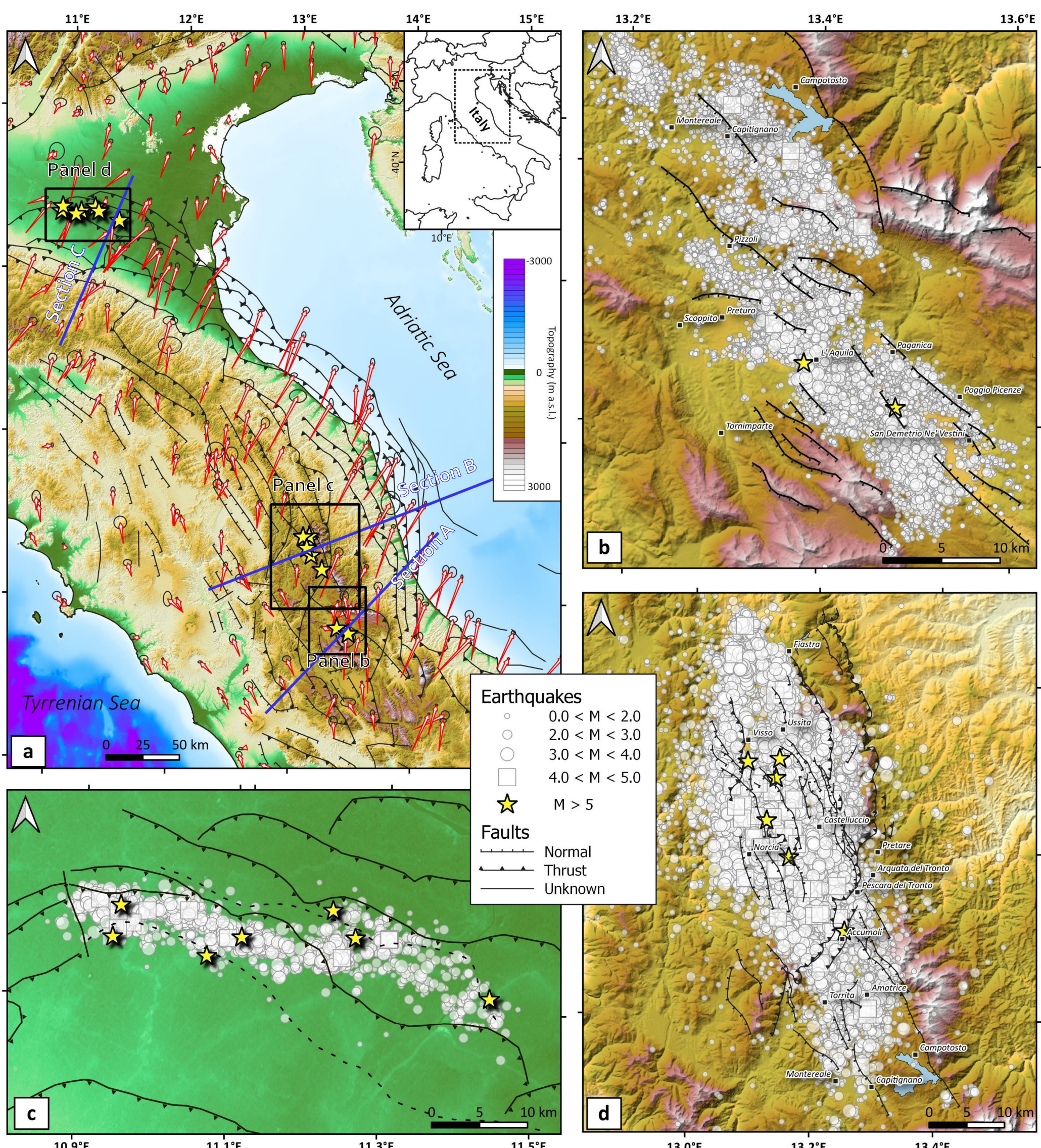


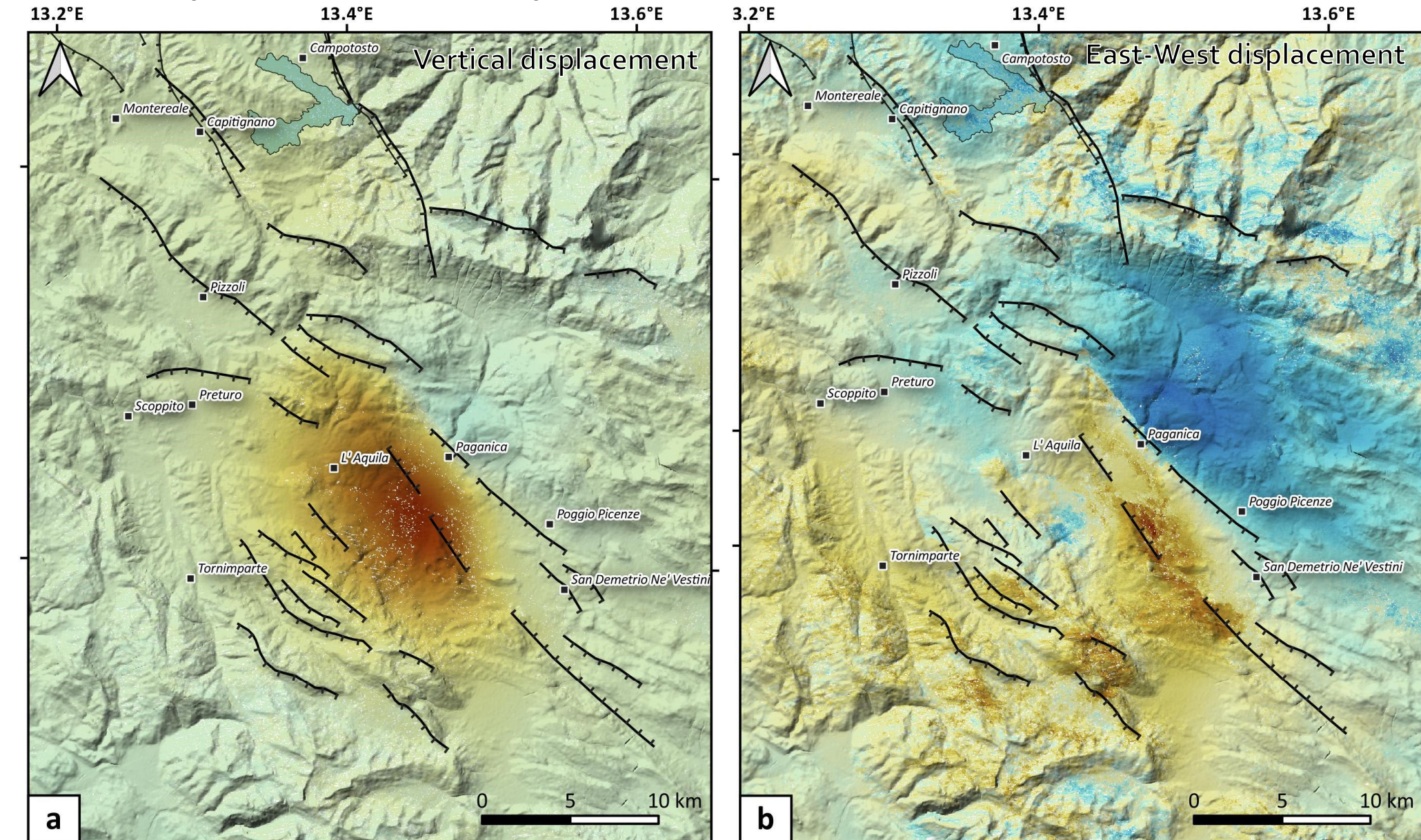
Figure 1. a) Location of the investigated earthquakes. The red arrows identify the horizontal interseismic ground velocities from GPS data (Mantovani et al., 2015); b) L'Aquila seismic sequence (Valoroso et al., 2013); c) Emilia Romagna seismic sequence (Govoni et al., 2013); d) Amatrice-Visso-Norcia seismic sequence (Chiarioluce et al., 2017).

## Data and methods

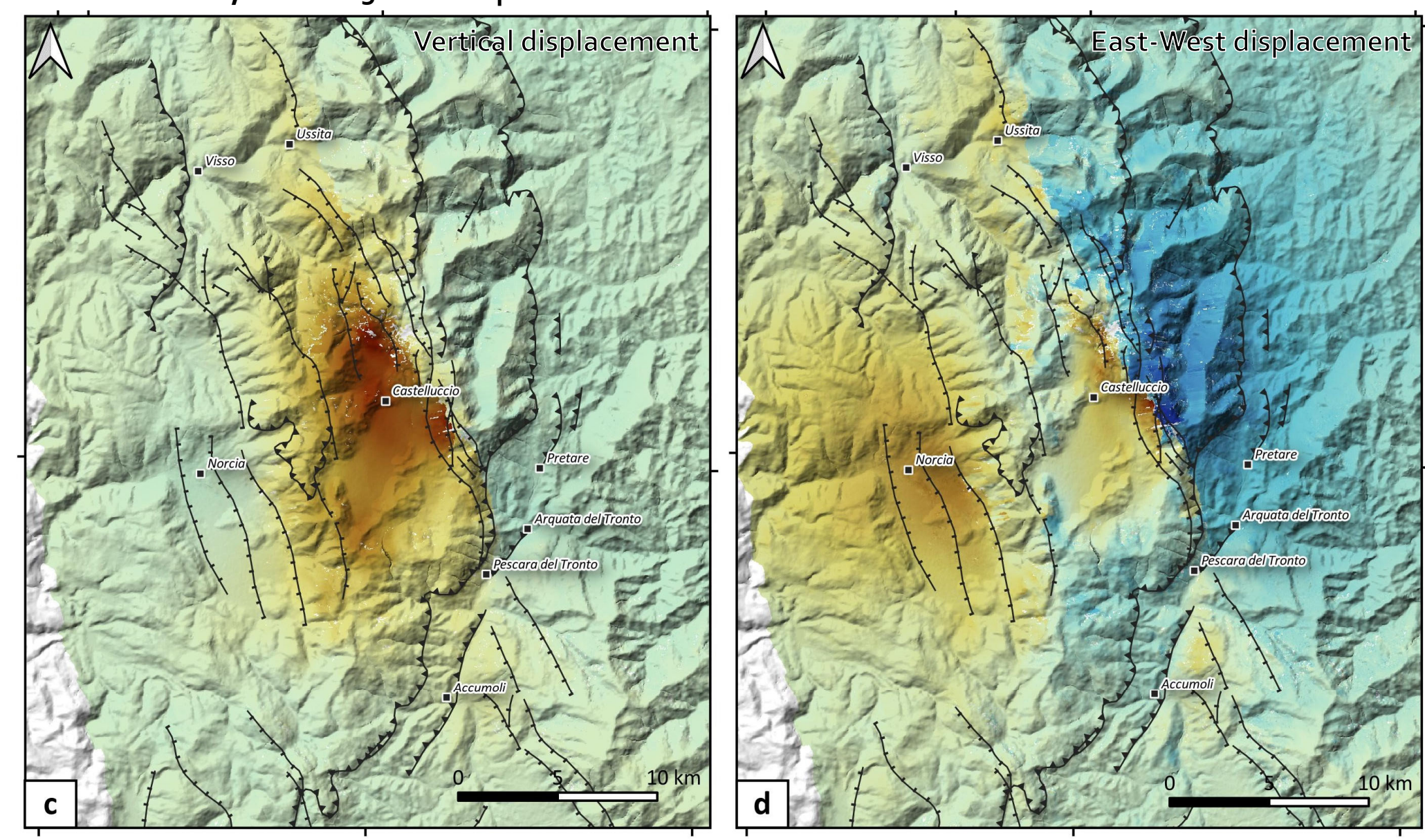
### InSAR data

Coseismic ground displacements are identified by means of Synthetic Aperture Radar Interferometry technique (InSAR). SAR data from the ENVISAT, ALOS-2 and RADARSAT satellite constellations are exploited to retrieve the ground displacements for the L'Aquila (Figure 2 a and b), Norcia (Figure 2 c and d) and Emilia Romagna (Figure 2 e) earthquakes, respectively.

### 2009 L'Aquila, Mw 6.1 earthquake



### 2016 Norcia, Mw 6.5 earthquake



### 2012 Emilia Romagna, Mw 6.0 earthquake

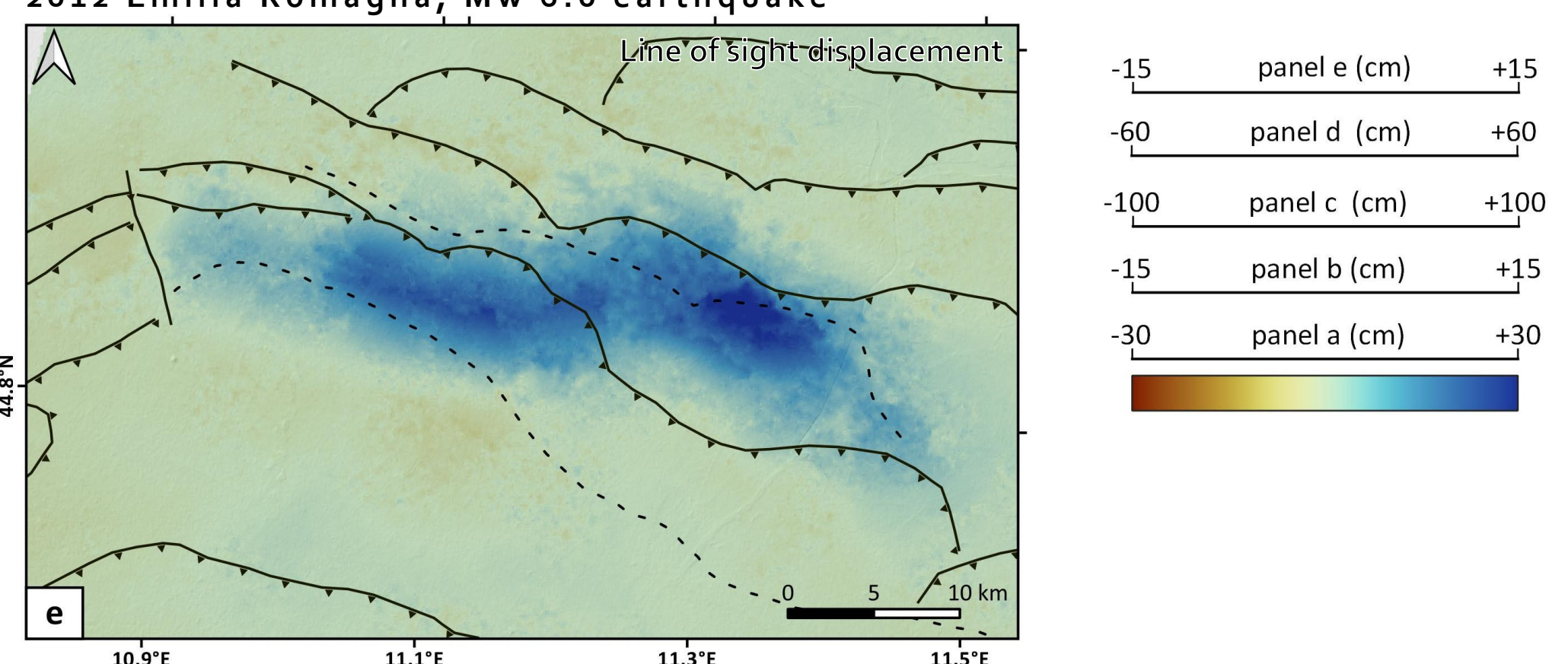


Figure 2. Results of the InSAR analysis for the three earthquakes in Figure 1. a) Vertical and b) East-West displacements from ENVISAT SAR data caused by the L'Aquila earthquake. c) Vertical and d) East-West displacements from ALOS-2 SAR data caused by the Norcia earthquake. e) Line of sight displacements along the RADARSAT descending orbit caused by the Emilia Romagna earthquake.

## Data and methods

### Numerical modeling

The model is developed to simulate typical extensional and compressional earthquakes including the forces acting during the interseismic period, i.e., the lithostatic load and the horizontal stress field (black horizontal arrows in Figure 3).

The model assumes a brittle upper crust where the fault is locked in the interseismic phase (red segment in Figure 3), and a ductile lower crust, where the fault is steadily shearing during both interseismic and coseismic stages (green segment in Figure 3).

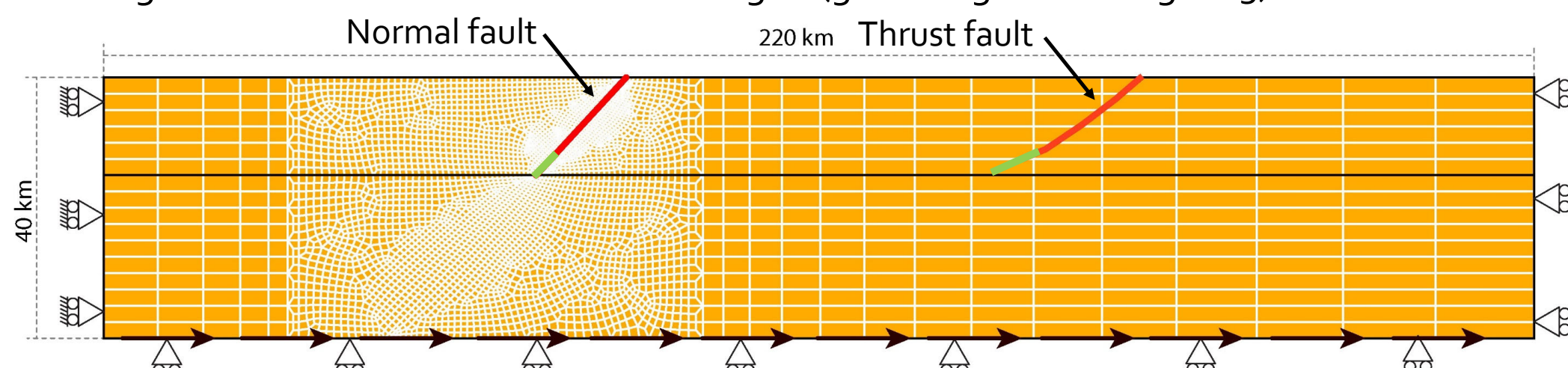


Figure 3. FEM setup for normal and thrust faulting. The black horizontal arrows represent the tectonic forces applied as a shear load (Finocchio et al., 2016). The fault is modelled as a contact interface. The upper part (red segment) is locked during the interseismic loading and is unlocked during the coseismic stage to simulate coseismic ground displacements (Doglioni et al., 2011).

## Results

The model setup is adjusted to simulate the interseismic and coseismic phases of the seismic events along the three cross sections in Figure 1a. The magnitude of the basal shear load (i.e., the tectonic loading) is calibrated in order to fit the coseismic InSAR ground displacements in Figure 2. The interseismic loading (Figure 4) produces horizontal strains compatible with those derived from GPS interseismic velocities (Figure 1a).

### Interseismic loading

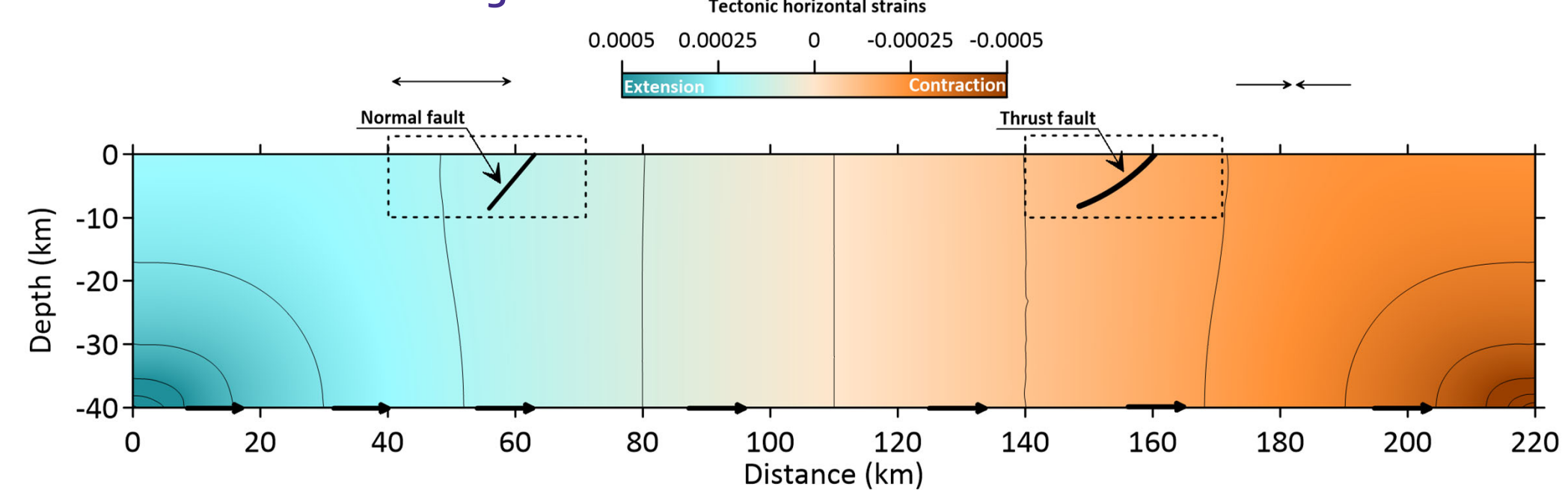


Figure 4. Horizontal strain field produced by the applied shear load, together with the gravitational load. Normal faults are located in extension areas, while thrust faults are located in contraction areas

The modeling provides evidence of interseismic dilatancy above the brittle-ductile transition at the bottom of the locked fault plane in the extensional tectonic setting. Coseismic fault motion is triggered by the hangingwall gravitational collapse that recovers most of the interseismic dilatancy formed almost orthogonal to the fault (Figure 5 and 6).

### L'Aquila earthquake

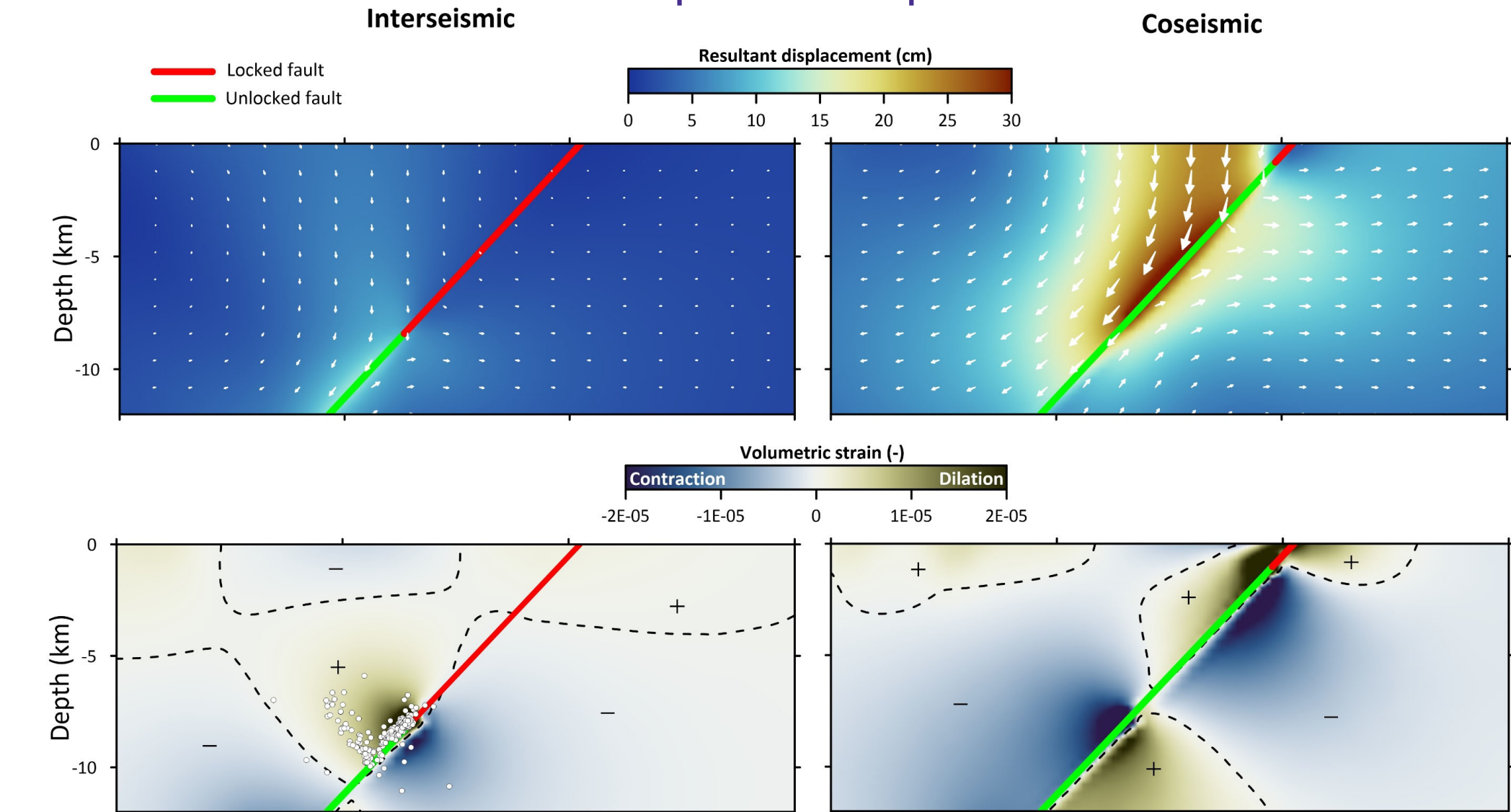


Figure 5. Simulation results for the 2009 L'Aquila earthquake (black dashed rectangle for normal fault in Figure 4). Upper panels: resultant displacements at the end of the interseismic and coseismic stages. Lower panels: volumetric strains at the end of the interseismic and coseismic stages (best fitted with InSAR data). The white dots locate the foreshocks before the Mw 6.1 event.

## Results

### Norcia earthquake

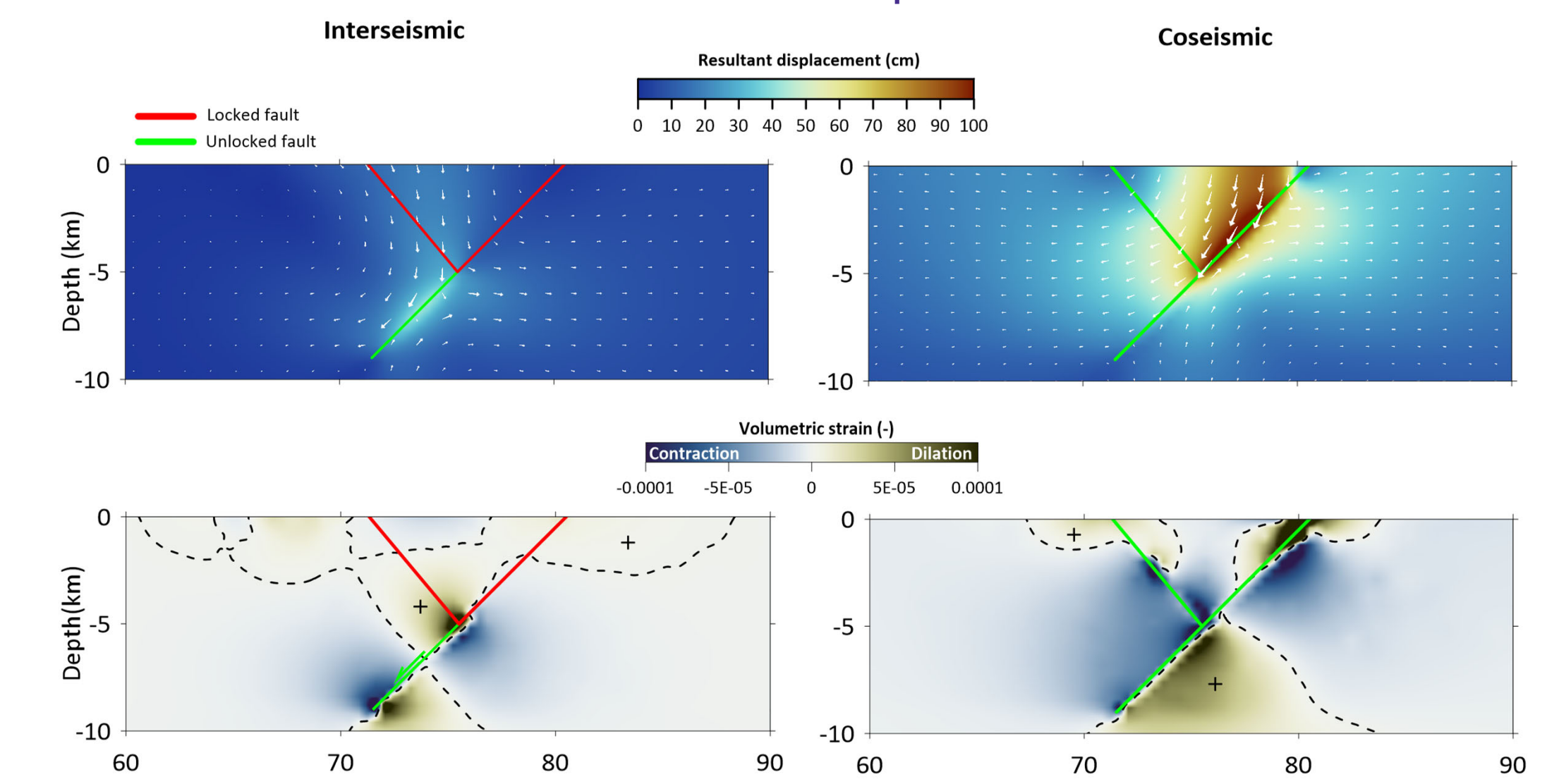


Figure 6. Simulation results for the 2016 Norcia earthquake (black dashed rectangle for normal fault in Figure 4). Upper panels: resultant displacements at the end of the interseismic and coseismic stages (best fitted with InSAR data). Lower panels: volumetric strains at the end of the interseismic and coseismic stages.

In contractional tectonic settings, the interseismic horizontal stress accumulates elastic energy in the crustal volume above the bottom of the locked fault; coseismic deformation recovers the elastic energy stored in the hangingwall (Figure 7).

### Emilia Romagna earthquake

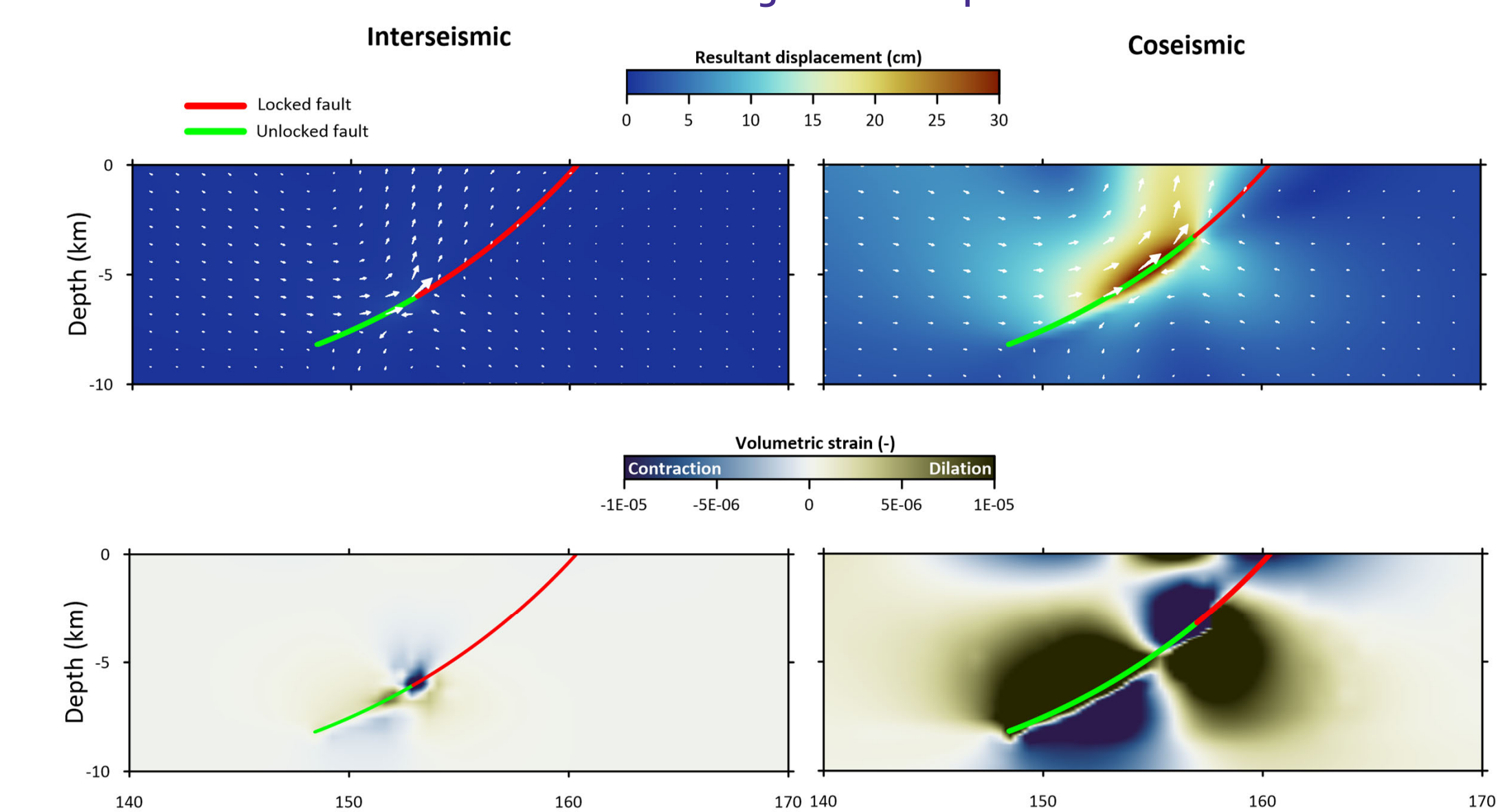


Figure 7. Simulation results for the 2012 Emilia Romagna earthquake (black dashed rectangle for thrust fault in Figure 4). Upper panels: resultant displacements at the end of the interseismic and coseismic stages (best fitted with InSAR data). Lower panels: volumetric strains at the end of the interseismic and coseismic stages.

## References

Chiarioluce, L.; Di Stefano, R.; Tinti, E.; Scognamiglio, L.; Michele, M.; Casarotti, E.; Cattaneo, M.; De Gori, P.; Chiarabba, C.; Monachesi, G.; Lombardi, A.; Valoroso, L.; Latorre, D.; Marzocchi, S. The 2016 Central Italy Seismic Sequence: A First Look at the Mainshocks, Aftershocks, and Source Models. *Seismol. Res. Lett.* 2017, 88, 757–771, doi:10.1785/S1523-0539-2016-0221.

Doglioni, C.; Barba, S.; Carminati, E.; Riguzzi, F. Role of the brittle-ductile transition on fault activation. *Phys. Earth Planet. Inter.* 2011, 184, 160–171, doi:10.1016/j.pepi.2010.11.005.

Finocchio, D.; Barba, S.; Basili, R. Slip rate depth distribution for active faults in Central Italy using numerical models. *Tectonophysics* 2016, 687, 232–244, doi:10.1016/j.tecto.2016.07.031.

Govoni, A.; Marchetti, A.; De Gori, P.; Di Bona, M.; Lucente, F. P.; Improta, L.; Chiarabba, C.; Nardi, A.; Margheriti, L.; Agostinetti, N. P.; Di Giovambattista, R.; Latorre, D.; Anselmi, M.; Ciaccio, M. G.; Moretti, M.; Castellano, C.; Piccinini, D. The 2012 Emilia seismic sequence (Northern Italy): Imaging the thrust fault system by accurate aftershock location. *Tectonophysics* 2014, 622, 44–55, doi:10.1016/j.tecto.2014.02.013.

Mantovani, E.; Viti, M.; Cenni, N.; Babbucci, D.; Tamburelli, C. Present Velocity Field in the Italian Region by GPS Data: Geodynamic/Tectonic Implications. *Int. J. Geosci.* 2015, 06, 1285–1316, doi:10.4236/ijg.2015.612103.

Valoroso, L.; Chiarabba, L.; Piccinini, D.; Di Stefano, R.; Schaff, D.; Waldhauser, F. Radiography of a normal fault system by 64,000 high-precision earthquake locations: The 2009 L'Aquila (central Italy) case study. *J. Geophys. Res. Solid Earth* 2013, 118, 1156–1176, doi:10.1002/jgrb.50130.